

## Recent Developments in Fast Neutron Radiography for the Interrogation of Air Cargo Containers

B.D. Sowerby<sup>1</sup>, N.G. Cutmore<sup>1</sup>, Y. Liu<sup>1</sup>, H. Peng<sup>2</sup>, J.R. Tickner<sup>1</sup>, Y. Xie<sup>2</sup> and C. Zong<sup>2</sup>

<sup>1</sup>CSIRO Minerals, Private Mail Bag 5, Menai, NSW 2234, Australia

<sup>2</sup>Nuctech Company Limited, 2/F Block A, Tongfang Building, Shuangqinglu, Haidan District, Beijing 100084 P.R. China

Email contact of main author: [brian.sowerby@csiro.au](mailto:brian.sowerby@csiro.au)

**Abstract.** There is a growing need to rapidly scan bulk air cargo for contraband such as illicit drugs and explosives. Ideally, cargo containers must be imaged without unpacking and with scan times of less than one minute. Fast neutron techniques are particularly attractive for screening cargo as they can be used to determine cargo composition. The Commonwealth Science and Industrial Research Organisation (CSIRO) has developed a scanner that combines fast (14 MeV) neutron and gamma-ray (or X-ray) radiography (FNGR). This direct, dual-beam radiography technique is much more efficient than methods that measure secondary radiation and has much better material discrimination sensitivity than the dual-energy X-ray technique. A full-scale prototype FNGR scanner was trialed by Australian Customs Service to screen incoming air cargo at Brisbane International Airport in 2005/6. The trial of the scanner demonstrated the material discrimination capability of the technology and its ability to make concealed organic materials more obvious. CSIRO and Nuctech Company Limited have recently developed a new version of the scanner suitable for commercial deployment that combines a 14 MeV fast neutron radiography system with dual-energy X-ray radiography. The X-ray system uses a 6 MeV LINAC X-ray source and Binocular Stereoscopic imaging with much better spatial resolution than the scanner trialed at Brisbane airport. The improved resolution, combined with binocular stereoscopic imaging, allows complex cargo images to be separated into multiple layers, making it easier to identify threat items. The first unit of the commercial scanner was recently commissioned in Beijing and initial results are presented.

### 1 Introduction

Security and border protection are key priorities for many countries around the world. There is a growing need for improved screening of air cargo. Potential scanning technologies need to be sensitive to a wide range of threats including explosive devices and materials, weapons, nuclear materials, narcotics and other contraband items. The volume of air cargo passing through airports usually precludes inspection methods that require the cargo to be deconsolidated into individual packages. A useful system must therefore be capable of rapidly scanning large numbers of air cargo containers without unpacking. Detecting a wide range of threats in large, consolidated cargos requires highly-penetrating radiation and an imaging system. Conventional high energy X-ray radiography is well suited to detecting items with distinctive shapes such as weapons. However finding small quantities of organic materials with ill-defined outlines such as narcotics or explosives is more difficult.

Air cargo is usually packed in lightweight aluminium air cargo containers (Unit Load Devices (ULDs)) or on pallets. Air cargo container sizes vary widely and contents range from single commodity loads through to consolidations containing many hundreds of different items. The most common ULDs have widths of about 1.4-1.6 m and a maximum weight of 1.6 tonnes. However some large ULDs and pallet cargos may weigh up to 6.8 tonnes and are up to 2.44 m wide<sup>1</sup>. Air cargo consignments are commonly limited by mass rather than volume, and loads are often heterogeneously distributed. Achieving a satisfactory level of mass screening of air

---

<sup>1</sup> Information on ULD and pallet dimensions is available on the websites of most air cargo handling companies. See for example <http://www.baworldcargo.com/configs/BAWCconfigurations.pdf>.

cargo is difficult because of the sheer volume of cargo, the time-critical nature of the movement of cargo, and the wide variation in cargo presentation for transport.

Only fast (high-energy) neutrons and high-energy X-rays or gamma rays have the required penetration for radiographic imaging of air cargo containers. A range of sophisticated X-ray imaging systems are now commercially available. These X-ray systems can provide high resolution 2-D density images of the contents of containers and are ideally suited to the detection of metallic objects with readily identifiable shapes such as firearms and other weapons. They are not well suited to the detection of illicit substances that have similar densities and shapes to many common substances.

For neutron techniques to be successfully applied to cargo screening they must firstly meet the industry requirements described above and secondly they must have significant advantages over the established and developing X-ray techniques. Fast neutron techniques are attractive for these applications as they have the required penetration, they interact with matter in a manner complementary to X-rays and they can be used to determine elemental composition.

Neutron interrogation techniques fall into two categories, namely radiography systems and systems that measure secondary radiation (neutrons or gamma rays). Fast neutron radiography techniques have the advantage of direct measurement of transmitted neutrons and are therefore more efficient and faster than techniques measuring secondary radiation such as neutron-induced gamma rays. There have been a number of excellent general reviews of neutron techniques for non-intrusive inspection [1,2,3]. In the present paper, discussion is confined to fast neutron radiography techniques and applications.

The present paper traces the development of the CSIRO fast neutron and gamma-ray radiography (FNGR) technique from laboratory prototypes [4] to full-scale prototype scanner tested at Brisbane International Airport [5] through to the recently developed commercial air cargo scanner.

## 2 Fast Neutron and Gamma-Ray (or X-Ray) Radiography (FNGR)

The transmission of monoenergetic fast neutrons through an object of density  $\rho$  and thickness  $x$  can be calculated using the equation:

$$I_n / I_n^0 = \exp(-\mu_n \rho x) \quad (1)$$

where  $I_n$  is the measured neutron intensity through the object,  $I_n^0$  is the measured neutron intensity with the object removed and  $\mu_n$  is the neutron mass attenuation coefficient. Similarly monoenergetic gamma-ray transmission can be written as:

$$I_g / I_g^0 = \exp(-\mu_g \rho x) \quad (2)$$

where  $I_g$  is the measured gamma-ray intensity through the object,  $I_g^0$  is the measured gamma-ray intensity with the object removed and  $\mu_g$  is the gamma mass attenuation coefficient.

The ratio,  $R$ , of the neutron and gamma-ray attenuation coefficients is:

$$R = \frac{\mu_n}{\mu_g} = \frac{\ln(I_n / I_n^0)}{\ln(I_g / I_g^0)} \quad (3)$$

The cross-section ratio  $R$  can therefore be determined directly from the measured neutron and gamma-ray transmissions without knowing the mass of material in the radiation beams. This ratio provides a powerful discriminator between different classes of material. FIG. 1 illustrates calculated values of  $R$  for a range of materials using 14 MeV fast neutrons and  $^{60}\text{Co}$  gamma-rays (average energy of 1.25 MeV).

The accurate measurement of  $R$  would in principle allow a wide variety of material classes to be directly identified. However, as the neutron and gamma-ray beam transmissions are measured along a line between the radiation source and detector, the measured  $R$  value is an average for the materials in front of each detector element. Various techniques, described later in this paper, have been developed to assist in the interpretation of images and in the estimation of the  $R$  value of individual objects.

Note that FNGR has much better sensitivity to material composition than dual high energy X-ray radiography. This is illustrated in FIG. 1, where the effective cross-section ratios for 6 and 3 MeV Bremsstrahlung radiation through  $50 \text{ gcm}^{-2}$  of material are shown, normalized to unity for polythene (see [6] for details of this calculation). In particular, FNGR offers the potential to discriminate between various classes of organic material, unlike dual energy X-ray techniques that effectively only offer the ability to discriminate between organic and metal objects [6].

### 3 Scanner Trial at Brisbane International Airport

#### 3.1 Scanner Design

Based on the successful demonstration of an early laboratory prototype FNGR scanner [4], the Australian Government supported the Australian Customs Service in the trialing of a prototype CSIRO Air Cargo Scanner at Brisbane International Airport. Features of this scanner have been described previously [5] and are summarized below:

- The scanner used a Thermo MF Physics A-711 14 MeV D-T neutron generator that can produce up to  $10^{10}$  neutrons/sec and a 185 GBq  $^{60}\text{Co}$  gamma-ray source. The generator was typically operated to produce about  $5\text{-}6 \times 10^9$  neutrons/sec.
- The radiation sources were mounted inside shielding and collimators defined separate narrow fan beams of neutrons and gamma-rays. The sources were located approximately 6.1 m from the 4.3 m high detector arrays.
- The cargo to be scanned passed through the tunnel of dimensions 2.7 m wide and 2.7 m high on a chain conveyor.
- The conveyor was typically operated at a speed of about 1-2 m/min to achieve scanning times of approximately 1-2 minutes per ULD once the leading edge of the container is at the scanner.
- The scanner used four columns of  $20 \times 20 \times 75$  mm plastic scintillator neutron detectors (704 detectors) and one column of  $10 \times 10 \times 50$  mm CsI(Tl) gamma-ray detectors (352 detectors), all with photodiode readout and operating in pulse counting mode.
- The density and  $R$  value images were combined by mapping the ratio  $R$  to the hue (colour) of the pixel. In the images, low  $R$  values (inorganic materials) were coloured blue, intermediate  $R$  values were coloured green and high  $R$  values (organic materials) were coloured orange, pink and red.

### 3.2 Cargo Radiation Exposure

Cargo passing through the scanner was briefly exposed to narrow fan-beams of neutrons and X-rays. Neutron dose rates and activation levels have been calculated for cargo passing through the scanner using the following assumptions:

- The cargo is scanned at 1 m per minute and passes down the centre of the scan tunnel.
- The cargo is an AKE ULD, filled with 40% metallic/60% organic materials by weight with a bulk density of  $0.25 \text{ g/cm}^3$ .
- The neutron source is operated at  $5 \times 10^9$  neutrons/sec.

The total neutron radiation equivalent dose received by the cargo during scanning was calculated to be approximately  $8 \text{ } \mu\text{Sv}$ . This is approximately the same radiation dose as the cosmic ray-induced natural background that would be received during about 90 minutes in an aircraft at 10,000 m altitude.

Air cargo scanners are required to comply with relevant regulations, particularly with regard to the irradiation of foods commonly present in air cargo. For example, in the USA and UK, the maximum irradiation energy is 10 MeV in the case of X-rays and 14 MeV in the case of neutrons. Also, in these countries, the dose imparted to the cargo must not exceed 0.01 Gy in the case of inspection devices that utilise neutrons and 0.5 Gy otherwise. The neutron dose delivered by the Brisbane scanner was over 1000 times lower than these regulations. Note that these regulations differ between countries.

### 3.3 Results of the Brisbane Trial

#### 3.3.1 Characterisation of air cargo at Brisbane International Airport

In late 2006 a statistical survey was carried out to determine the distribution of loads in incoming cargo passing through the prototype scanner Brisbane [6]. Overall, about 50% of cargo was loaded into ULDs and 50% on pallets.

From the per-pixel attenuation histograms for 14 MeV neutron and cobalt-60 gamma-ray (1.25 MeV average energy) transmissions, the distribution in mass-per-unit-area was calculated for different classes of cargo [6]. Based on these results, a scanner using radiation capable of penetrating through  $100 \text{ g/cm}^2$  would be able to image through 99.6% of the area of an average air cargo ULD. A scanner using radiation capable of penetrating through only  $50 \text{ g/cm}^2$  would be able to image through 87% of the area of an average air cargo.

#### 3.3.2 Detection capability and speed

The installation at Brisbane International Airport allowed the technology and associated business processes to be tested in a real time operational environment. The trial of the scanner at Brisbane was critical to understanding the potential of the technology and to show up both its strengths and areas that need further development. Strengths included the material discrimination capability of the technology, its ability to make hidden organic materials more obvious and the scanning speed. Consolidated cargo was scanned in less than two minutes once the cargo is at the scanner, thus allowing high volumes of cargo to be screened rapidly.

Comparative tests against two commercial single-beam X-ray scanners on a representative selection of air cargo showed that the neutron scanner had a detection capability comparable to the best of the available X-ray scanners, despite having significantly lower spatial resolution and without the multi-view capabilities of one of the X-ray systems. It was assessed that, with improved spatial resolution (5 mm detectors or smaller) and multi-view capability, the CSIRO Air Cargo Scanner has the potential to significantly outperform current commercial X-ray air cargo scanners.

## 4 Developments using the Reference Scanner

During and following the development of the Brisbane scanner, CSIRO also designed and commissioned a second prototype system, designated the Reference Scanner, at our Lucas Heights Laboratory [5]. The Reference Scanner was used to demonstrate the technology, to conduct research and development of potential improvements and to assess other potential applications.

### 4.1 Improved resolution

The Reference Scanner was used to assess and compare techniques for improving spatial resolution, including super-resolution [7] and reducing detector sizes. Laboratory trials on the upgraded Reference Scanner have shown that the use of small (5×5mm) gamma detector elements provides better spatial resolution than super-resolution methods using the 10 mm detector elements used in the Brisbane scanner. For the 20×20mm neutron detector elements, super-resolution provided an adequate improvement in resolution and maintained the detector count rates necessary to allow rapid scanning. The resulting higher resolution images were found to be a significant aid in understanding complex, high-clutter cargos.

The scans of a resolution test plate and a motorbike (FIG. 2) illustrate the improved resolution obtained. These images provide a good indication of the overall imaging capabilities of the scanner. The metal frame and engine of the bike show up blue in the composition image; whereas the fuel in the petrol tank, rubber tyres, plastic seat, lights etc show up orange. The oil in the sump (immediately above the kickstand), when averaged together with the metal in the same path, shows as a green patch.

### 4.2 Cargo Images from the Reference Scanner

To trial the Reference Scanner, a range of cargos was prepared that broadly represented the types of items traveling through Australian airports. These cargos contained items such as heavy industrial machinery, electronics goods, household and office effects and fresh and preserved foodstuffs. A variety of real and simulated contraband items were concealed in these cargos which were then scanned using the Reference Scanner. The suspect items were detected and identified on the basis of their shape and  $R$  value.

A single ULD containing a wide range of items was also scanned and scans of this cargo, without concealed contraband, are shown in FIG. 3. The images illustrate the spatial resolution of the scanner and its ability to distinguish between different material categories.

### 4.3 Special nuclear materials

The detection of small quantities of special nuclear materials such as  $^{235}\text{U}$  and  $^{239}\text{Pu}$  being illicitly shipped inside air and sea freight is a problem receiving considerable attention. The

ease of shielding gamma rays emitted naturally by these materials means that active interrogation methods are likely to be required for efficient detection.

The  $R$ -values of high atomic number elements such as lead, tungsten, uranium and plutonium are approximately a factor of two lower than those of the nearest common materials such as iron, steel and copper. We have conducted a study using our reference laboratory scanner [8], where pieces of tungsten and depleted uranium were used as nuclear material surrogates. These were scanned hidden inside air freight containers holding a range of different cargos. The resulting neutron and gamma-ray images were analysed using a modified version of the dual-energy decomposition technique [9]. As nuclear and shielding materials lie at the extreme end of the  $R$ -value range, it is possible to decompose the composite neutron/gamma-ray image into two images, one containing just the materials of interest and the second containing all other items in the cargo. This demonstrated that the FNCR method is a potentially effective tool in locating smuggled nuclear materials.

## **5 Commercial Air Cargo Scanner**

In 2007, CSIRO signed a joint venture agreement with Nuctech Company to develop and commercialise a new scanner incorporating CSIRO's neutron technology and Nuctech's X-ray technology. The first commercial unit of the new air cargo scanner (the Nuctech AC6015XN Air Cargo Scanner) has been commissioned in Beijing and is undergoing a program of trials to demonstrate the technology.

### **5.1 Overall Design and Shielding**

The AC6015XN scanner has been designed to provide lower overall hardware cost, significantly smaller footprint (approximately 40% of the Brisbane prototype design), modular design for rapid installation and a more flexible cargo handling system. In particular, the neutron source is shielded using water-filled tanks, rather than concrete blocks as used for both the Brisbane and Reference Scanners.

The AC6015XN scanner combines dual energy X-ray radiography and fast neutron radiography technology as shown in FIGS. 4 and 5. The evaluation of the Brisbane Airport scanner showed that higher resolution and multi-view capacity would greatly assist the detection of threat items. The new scanner uses two arrays of  $5 \times 10$ mm X-ray detectors and incorporates binocular stereoscopic X-ray radiography to provide the operator with X-ray images from two different view angles. This information is used to carry out a tomographic analysis of cargo (see section 5.5). The fast neutron image is fused with the X-ray data to provide composition information. The cargo transportation system is similar to that used in the Brisbane scanner with a chain conveyor carrying cargo smoothly through the scanning tunnel.

### **5.2 Neutron System**

The AC6015XN scanner uses the same neutron generator as that used in the Brisbane scanner but with a new D-711 digital controller. The digital controller allows software based on/off control that does not require scanner operators to get involved in complex neutron generator start-up and control procedures.

The scanner uses similar neutron detector arrays to those developed by CSIRO for the Brisbane model. The neutron detectors are configured to be parallel to one X-ray beam. Four columns of 20×20 mm neutron detectors with offset detector elements are used and mathematical reconstruction techniques (super-resolution methods) employed to calculate an image at higher resolution than the pixel size.

### 5.3 Dual Energy X-Ray Material Discrimination

The AC6015XN scanner uses a Nuctech 6/3MeV dual energy LINAC. The X-ray output is collimated into two vertical fan-beams separated by an angle of 9°. Alternate pulses from the LINAC are emitted at high and low energies. Compared to using a <sup>60</sup>Co radioisotope source, the advantages of using a LINAC include higher penetration, higher source intensity, improved image quality and improved safety as the source can be switched off. The penetration of 3 and 6 MeV Bremsstrahlung X-rays is larger than that of 14 MeV neutrons for all materials of atomic number less than about 15 (FIG. 6). The dual-energy X-ray system can be used to discriminate between organics and metals but its ability to discriminate different classes of organic materials is very limited. However, its material discrimination is useful when scanning thick organic cargo through which 14 MeV neutrons cannot penetrate.

The AC6015XN scanner uses X-ray detectors previously developed by Nuctech. The detectors use 5×10mm CsI(Tl) scintillators in a folded configuration on the side and top of the tunnel through which cargo passes. Current mode counting is used for the X-ray detectors and readout is every 5 mm of travel.

### 5.4 Beam Hardening Correction

The  $R$  value calculations presented in section 2 are only valid for monoenergetic neutron and gamma-ray beams. The Bremsstrahlung X-ray beams emitted by the LINAC source cover the full energy range up to the incident electron energy (3 or 6 MeV). This leads to beam-hardening effects, where the energy spectrum of transmitted X-rays shifts to higher energies with increasing material thickness. In turn, this causes the attenuation of broad-energy X-ray beams to deviate from a simple Beer-Lambert exponential law and means that  $R$  values calculated using equation (3) will no longer be independent of material thickness.

FIG. 7 plots the negative logarithm of the calculated attenuation of 3 MeV Bremsstrahlung X-rays through various materials as a function of their mass per unit area. We find that to an excellent approximation, the shapes of the attenuation curves agree to within a multiplicative, material-dependent constant. This means that a single, material-independent, beam-hardening correction curve can be used and the resulting  $R$  value determinations are independent of thickness. The biggest variations of  $R$  value with thickness are observed for heavy metals (for example, lead), but the  $R$  values of these materials can still be readily distinguished. Following this procedure, the  $R$  values of different materials are shifted slightly from their theoretical values for a true monoenergetic source, but this effect can be easily accounted for. FIG. 8 shows a scan of a selection of common materials and compares their measured and theoretical  $R$  values.

### 5.5 Binocular Stereoscopic Imaging

The single greatest obstacle to the detection of small threat items in air cargo is image complexity. Air cargo is generally significantly more cluttered than sea freight and this places heavy demands on analysts particularly when the time for image interpretation is short.

Multiple views of the same cargo can prove very advantageous in resolving this complexity. The conventional approach is to use dual radiation sources and detector arrays to provide orthogonal views, usually from the side and from above. However, our experience is that operators of these systems generally struggle to assimilate two very different views when they were only given a short time to analyse images.

A simpler alternative is to use binocular stereoscopic imaging [10]. The system implemented in the AC6015XN scanner utilizes a single X-ray source and two folded X-ray detector arrays (FIG. 5). This system allows complex cargo images to be separated into multiple layers, making it easier to identify threat items.

## 5.6 Image Processing and Display System

From the raw neutron and X-ray images, a suite of new images are calculated for user analysis. The primary output combined both the neutron and 3 MeV X-ray data to produce a coloured image that shows shape, density and composition information. Secondary outputs are the 6 MeV X-ray grey-scale images, which offer maximum penetration through thick cargos, and the segmented binocular stereoscopic images which shows the cargo as a series of depth-based 'layers'.

The images are corrected for dead-time (neutron scan) and ADC dark-noise (X-ray scans), non-functioning detector elements, geometric distortion and variations in the output intensity of the X-ray and neutron sources. The X-ray and neutron images are then accurately registered and non-linear spatial filters are applied to simultaneously improve sharpness whilst reducing statistical "noise" or speckle [11].

Images are displayed using custom image visualisation software, designed to allow image analysts to rapidly manipulate and interpret the images to detect contraband items. In addition to the usual display functions (brightness and contrast adjustment, histogram equalisation and inverse mode), the software allows the user to rapidly compare different views of the same cargo. A material identification tool indicates possible substances that are compatible with the  $R$  value of a point in the image (selected using the computer mouse). To help resolve the problem of overlapping items, a background stripping tool can be used to mathematically remove over- or underlying material and provide a better  $R$  value estimate for an object of interest.

The AC6015XN scanner has been evaluated on a range of test objects and cargos. FIGS. 8-10 show some of the processed, full-colour images obtained.

## 6 Potential Application to the Scanning of Sea Freight

Both fast neutrons and high energy X-rays have sufficient penetration for air cargo screening. However, the penetration of fast neutrons depends much more on atomic number than it does for high energy X-rays (FIG. 6) and the most significant obstacle to the application of the FNCR technique to the scanning of sea freight is the neutron penetration required to image through thick, organic cargos.

Based on maximum mass and cross-sectional area of various air cargo containers, the average mass per unit area of the largest pallets used for air cargo (which comprise about 33% of air cargo through Brisbane International Airport [6]), is roughly equivalent to the most common



40 ft sea containers. However, smaller ULDs typically have a maximum average mass per unit area of about 60% of a 40 ft sea container.

Data is readily available on the dimensions and maximum mass loadings for both sea and air cargo. The maximum average MPUA is  $158 \text{ g/cm}^2$  for fully laden 20 ft containers and  $93 \text{ g/cm}^2$  for the most common 40 ft containers (comprising about 70% of sea cargo imported into the USA). However, there is limited data on actual mass loadings. To our knowledge the best data that is available on sea cargo is that presented by Descalle et al [12]. These authors show that for sea cargo imported into the USA, the mean cargo mass per unit area is about  $50 \text{ g/cm}^2$  and only 8.5% of the cargo has an average bulk mass per unit area greater than  $100 \text{ g/cm}^2$ . Based on this data, a reconfigured FNCR scanner similar in design to the AC6015XN has sufficient penetration to be used for the interrogation of the large majority of sea cargo containers.

## 7 Summary

CSIRO has invented and demonstrated a new technique for imaging air cargo. A prototype scanning system based on this technology has been the subject of an extensive field trial by Australian Customs at Brisbane International Airport. The first commercial scanner combining CSIRO neutron and Nuctech X-ray technologies was recently commissioned at Nuctech's factory in Beijing.

Existing bulk scanning technologies use high-energy X-rays to detect distinctive metal objects such as weapons, but ill-defined organic materials such as drugs and explosives, are harder for them to detect. The AC6015XN commercial Air Cargo Scanner uses neutron and X-ray beams to show not only the shape, but the composition of materials inside the cargo. This helps with image analysis, particularly in the detection of organic materials with ill-defined shapes such as concealed narcotics and explosives.

Compared to dual high-energy X-ray scanning techniques, fast neutron/X-ray radiography offers the additional significant advantage of discriminating between a wide range of organic materials. This improved discrimination assists operators in interpreting the complex and often highly cluttered cargo images that result from scanning air cargo and has the potential to facilitate in the detection of narcotics, explosives and other organic threat materials.

## 8 Acknowledgments

The CSIRO authors gratefully acknowledge the financial support and assistance of the Australian Customs Service and the Department of Prime Minister and Cabinet in the development and testing of the Brisbane Airport and Reference Scanners.

## 9 References

1. GOZANI, T., "A review of neutron based non-intrusive inspection technologies", in Conf. on Technology for Preventing Terrorism, Stanford, 12-13 March 2002.
2. BUFFLER, A., "Contraband detection with fast neutrons", *Radiation Physics and Chemistry* 71 (2004) 853
3. RUNKLE, R.C., WHITE, T.A., MILLER, E.A., CAGGIANO, J.A. AND COLLINS, B.A., "Photon and neutron interrogation techniques for chemical explosives detection in

- air cargo; A critical review”, Nucl. Instr. And Meth. A (2009), doi: 10.1016/j.nima.2009.02.015
4. EBERHARDT, J.E., RAINEY, S., STEVENS, R.J., SOWERBY, B.D. AND TICKNER J.R., “Fast neutron radiography scanner for the detection of contraband in air cargo containers”, Applied Radiation and Isotopes 63 (2005) 179-188.
  5. EBERHARDT, J.E., LIU, Y., RAINEY, S., ROACH, G.J., STEVENS, R.J., SOWERBY B.D. AND TICKNER, J.R., “Fast neutron and gamma-ray interrogation of air cargo containers”, (International Workshop on Fast Neutron Detectors, Cape Town, 3-6 April 2006), Proceedings of Science (FNDA2006) 092 (<http://pos.sissa.it>)
  6. LIU, Y., SOWERBY, B.D. AND TICKNER, J.R., “Comparison of neutron and high energy X-ray dual-beam radiography for air cargo inspection”, Applied Radiation and Isotopes Applied Radiation and Isotopes 66(2008)463-473
  7. FARSIU, S., ROBINSON, D., ELAD, M., MILANFAR, P., “Advances and challenges in super-resolution”, Int. J. Imaging Syst. Technol., 14 (2004) 47-57.
  8. EBERHARDT, J., LIU, Y., ROACH, G., SOWERBY, B. AND TICKNER, J., “Feasibility Study of the Detection of Special Nuclear Materials in Air Cargo Using Fast-Neutron/Gamma-ray Radiography”, 2007 IEEE Nuclear Science Symposium (NSS) and Medical Imaging Conference, Honolulu, Hawaii (October 28 to November 3, 2007)
  9. DOBBINS J.T., WARP R.J., Dual-energy methods for tissue discrimination in chest radiography. In: Samei E., Flynn M.J., eds. Advances in Digital Radiography: RSNA Categorical Course in Diagnostic Radiology Physics. Oak Brook, Ill: RSNA; 2003:173-179
  10. EVANS, J.P.O., Stereoscopic imaging using folded linear dual-energy x-ray detectors, Meas. Sci. Technol. 13(2002)1388-1397
  11. LIU, Y. AND TICKNER, J.R., “Image processing and display systems for the CSIRO Air Cargo Scanner”, IEEE Nuclear Science Symposium, San Diego, California (2006) 77-81
  12. DESCALLE, M, MANNAT, D. AND SLAUGHTER, D., “Analysis of recent manifests for goods imported through US ports”, UCRL-TR-225708, 2006

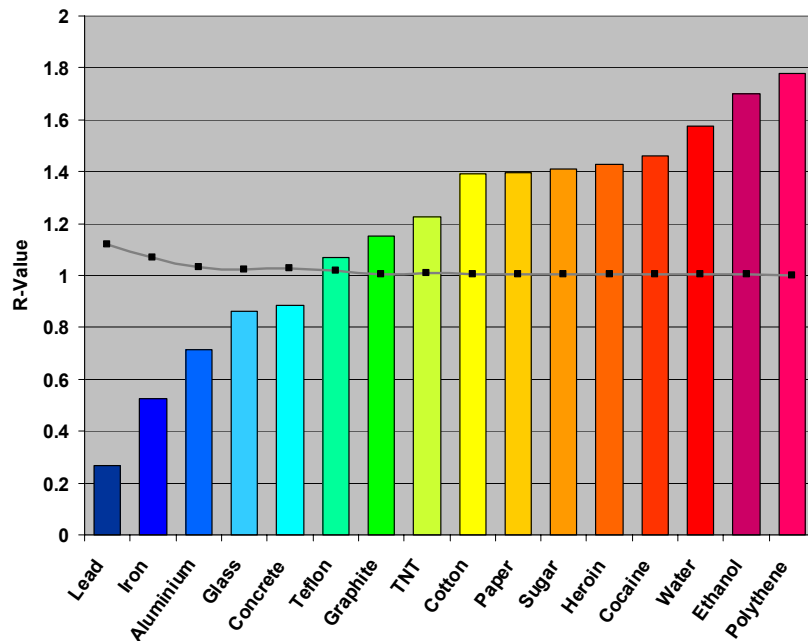


FIG. 1. Calculated  $R$  values for a range of materials, using 14 MeV neutrons and  $^{60}\text{Co}$  gamma rays. The solid line shows effective cross-section ratios for 6 and 3 MeV Bremsstrahlung for 50 g/cm<sup>2</sup> thick objects, normalised to unity for polythene.

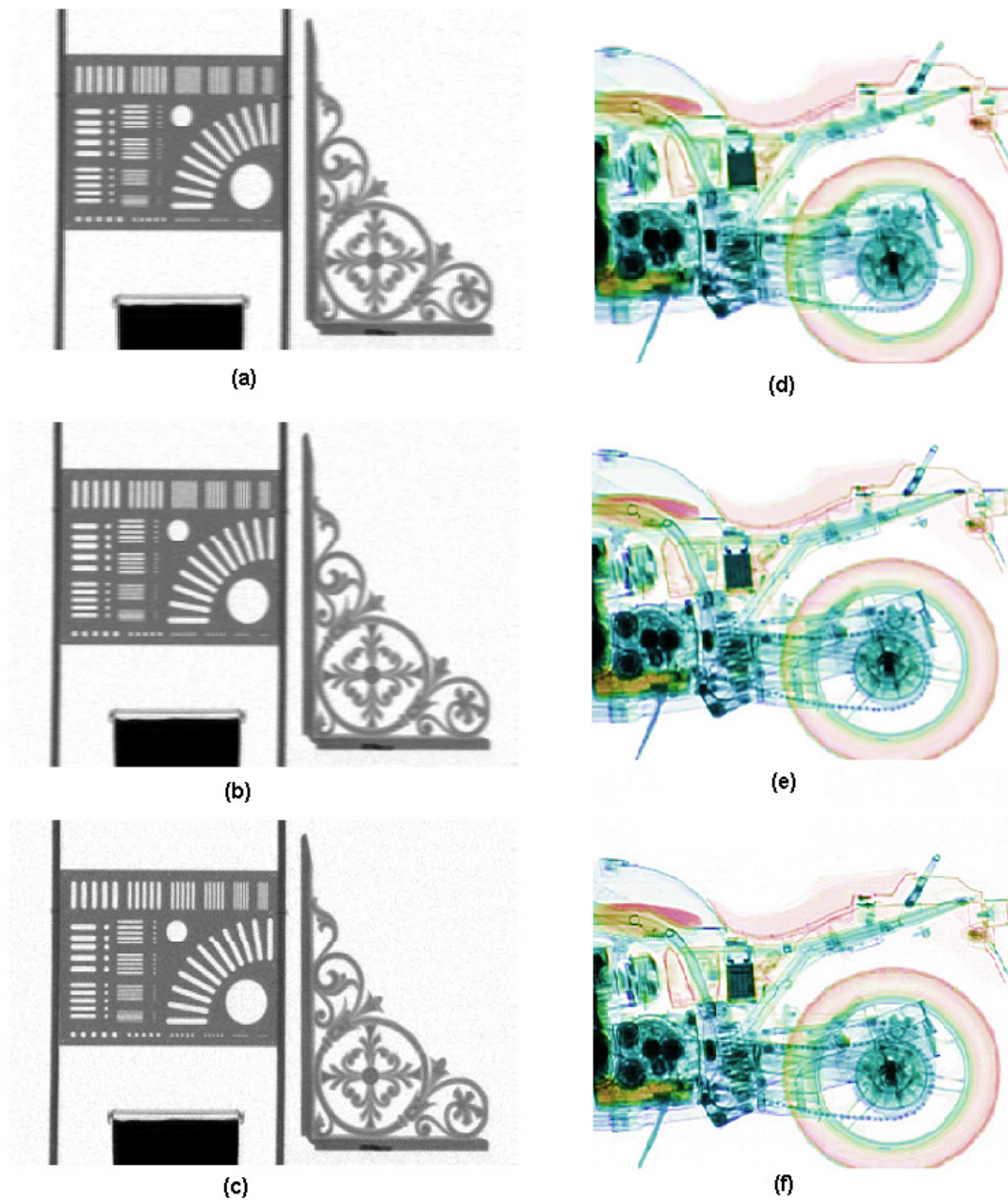


FIG. 2. Images obtained with the Reference Scanner showing resolution changes. Resolution plate and iron lace scans: (a) with 10x10mm gamma detectors; (b) with interleaved 10x10mm gamma detectors; and (c) with 5x5mm gamma detectors. Part of motorbike scan: (d) with 10x10mm gamma detectors; (e) with interleaved 10x10mm gamma detectors; and (f) with 5x5mm gamma detectors.

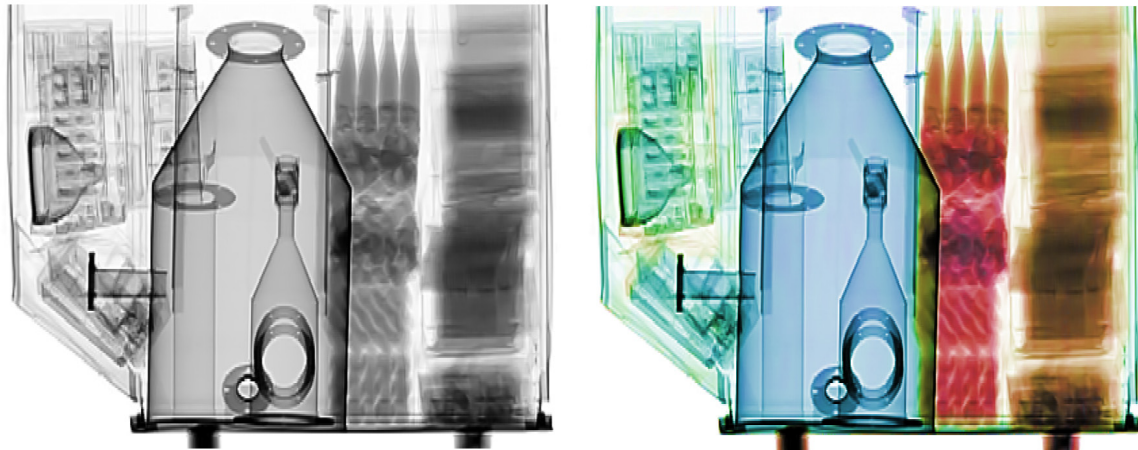


FIG.3. Cargo images from the Reference Scanner. The left-hand image is a gamma-ray scan and the right-hand image is a combined neutron and gamma scan of a ULD loaded with mixed cargo. From left-to-right, the cargo contains assorted computer equipment, heavy steel industrial items, mixed boxes of food stuffs (including bottled drinks, frozen meat and fish, boxed apples) and boxes containing office files and papers.

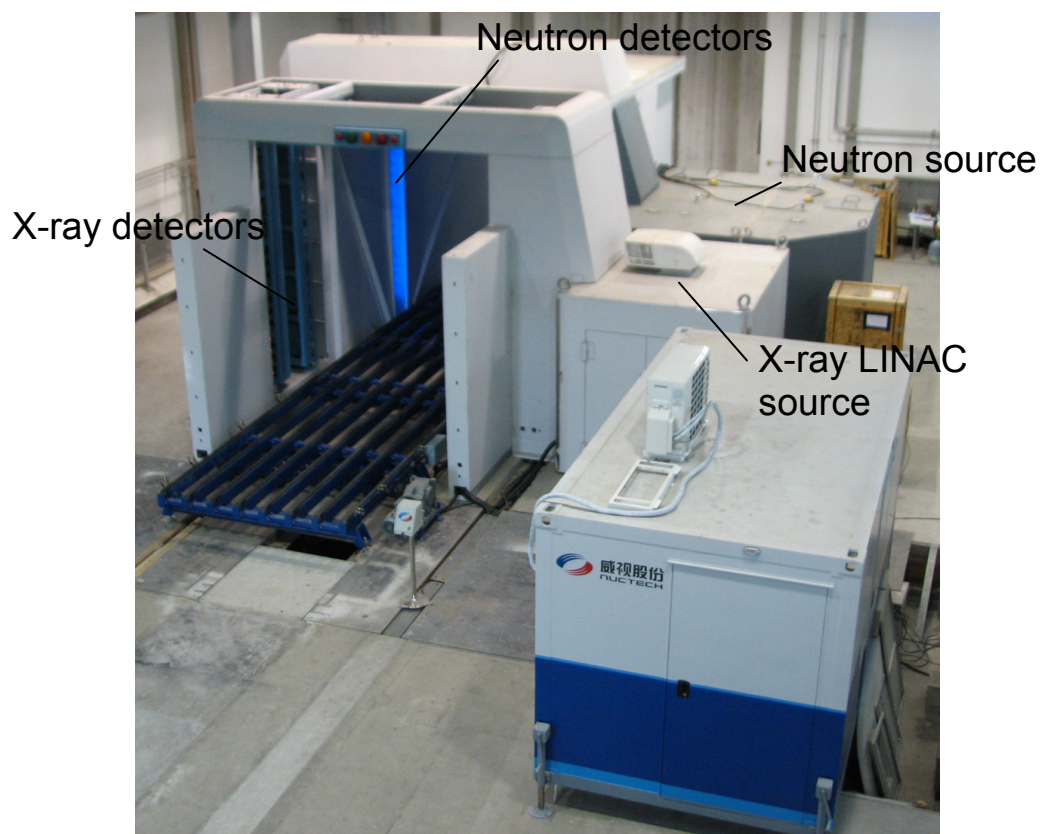


FIG. 4. Photograph of the first commercial unit of the new air cargo scanner developed by Nuctech and CSIRO (the Nuctech AC6015XN Air Cargo Scanner) that has been recently commissioned in Beijing.

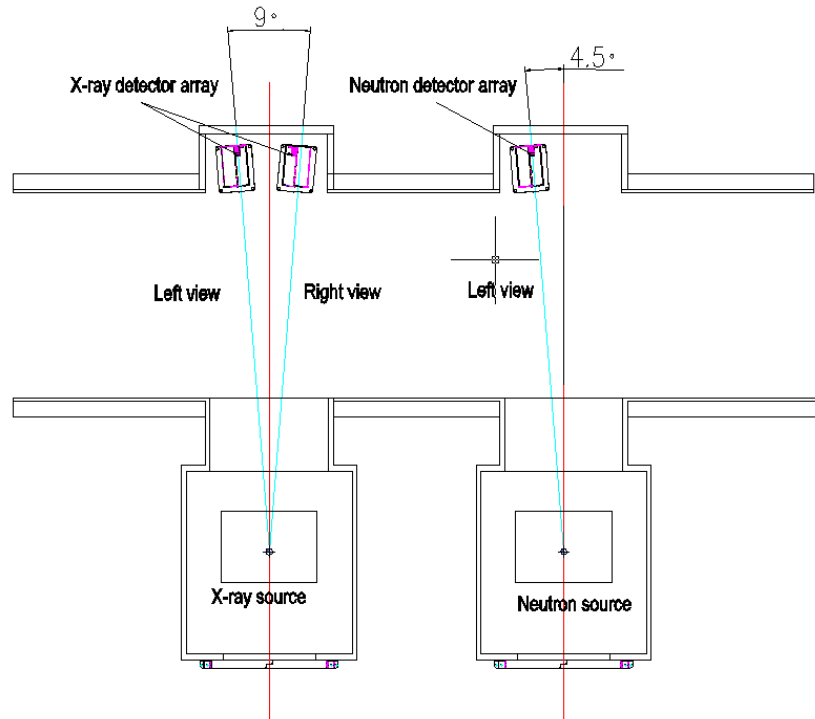


FIG. 5. Schematic plan view of the layout of the X-ray and neutron beams in the AC6015XN scanner.

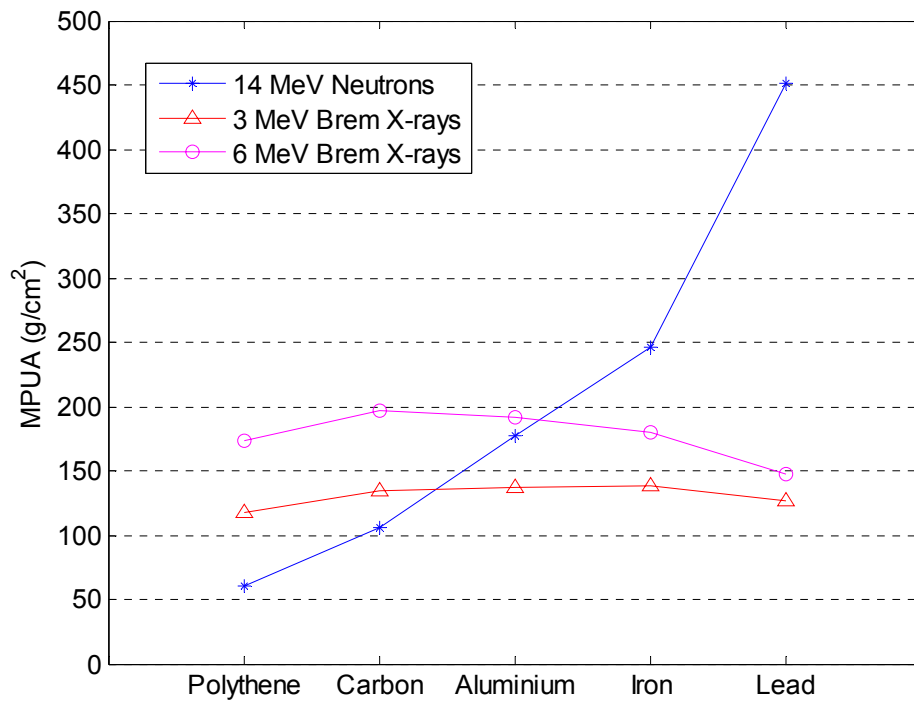


FIG. 6. Mass per unit area (MPUA) for 0.1% transmission of 14 MeV neutrons and 3 and 6 MeV Bremsstrahlung X-rays through five materials.

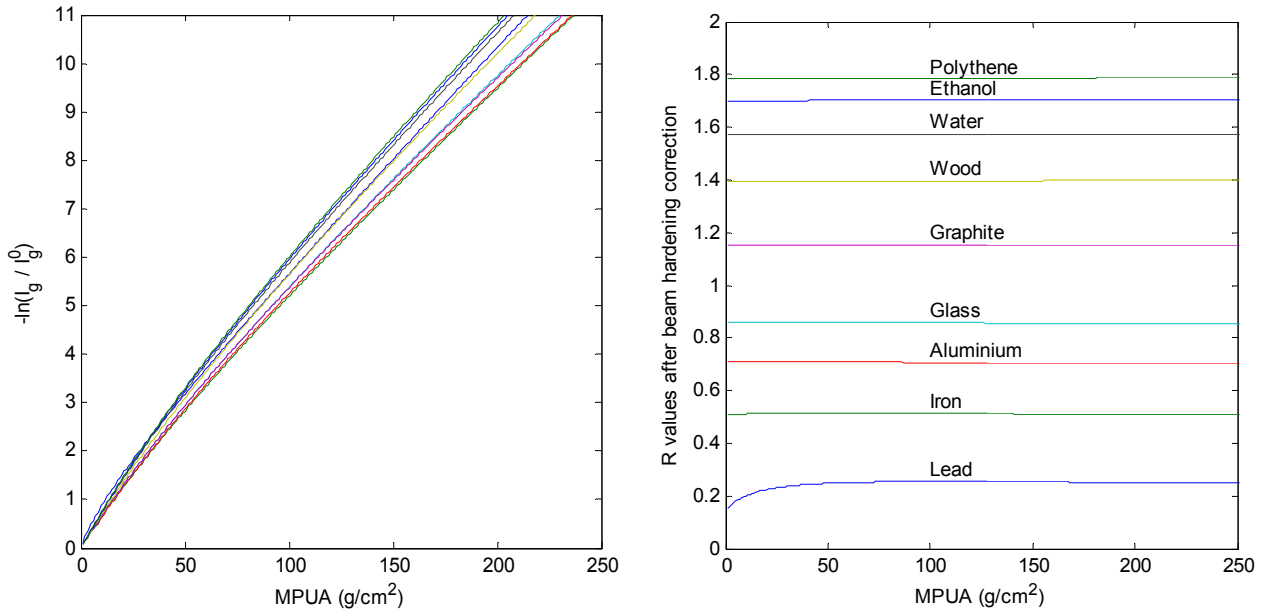


FIG. 7. Left: Transmissions (plotted on negative log scale) of 3 MeV Bremsstrahlung X-rays through various materials as a function of thickness (MPUA). Right: R values of 14 MeV Neutrons and 3 MeV X-rays (corrected for beam hardening) for the same materials as a function of thickness.

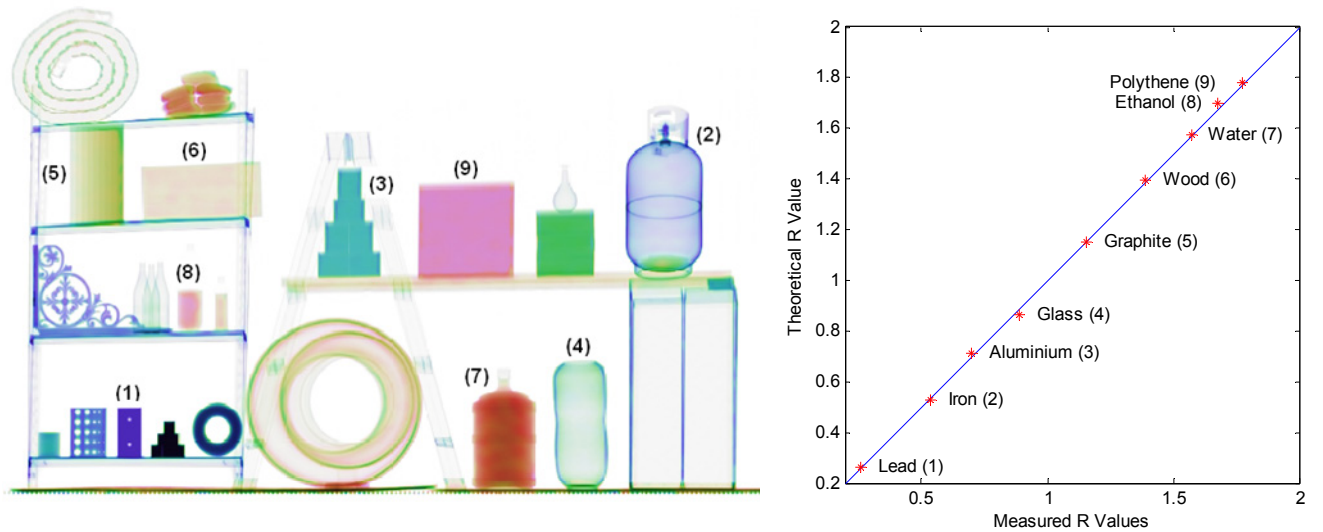


FIG. 8. Scan of a selection of material samples and common objects arranged on shelves, etc in the AC6015XN scanner. The graph on the right compares measured and theoretical R-values (standard deviation = 0.0154, correlation coefficient = 0.9997).

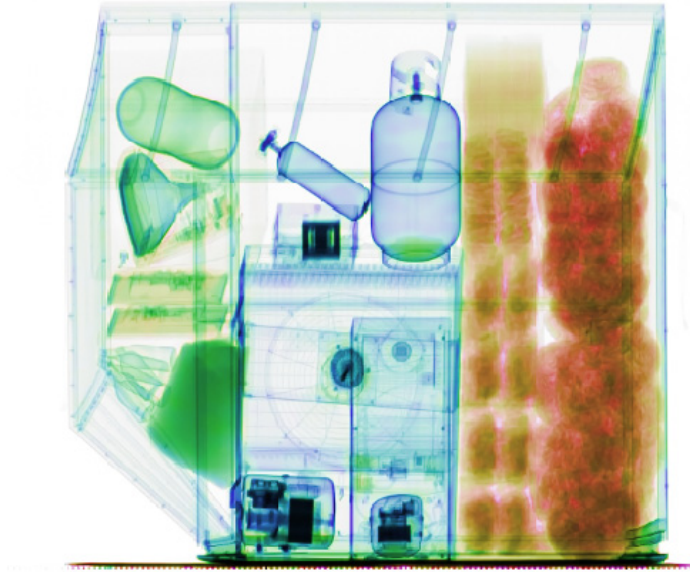
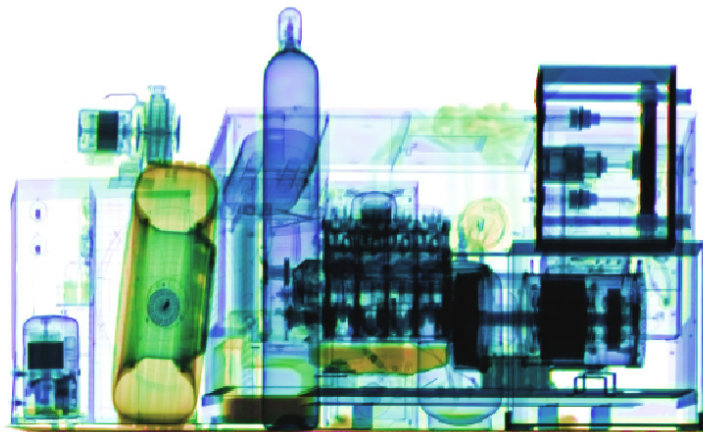
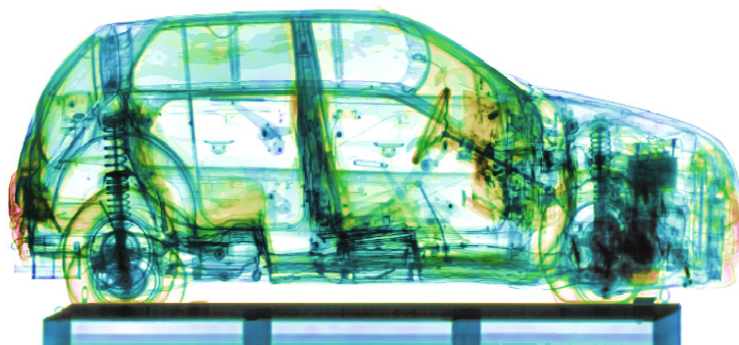


FIG. 9. Combined neutron and X-ray scan of ULD loaded with mixed cargo in the AC6015XN scanner. The cargo contains computer monitors (CRT and LCD), a porcelain vase, glass bottles and a sack of industrial chemicals (left), air conditioners and gas bottles (middle), and vegetables (right).



(A)



(B)

FIG. 10. Combined neutron and X-ray scan of (A) diesel generator, gas bottles, large truck wheel, pumps, and other machines; (B) a small car on a steel platform.